Cell Reports

Article

Adult pancreatic islet endocrine cells emerge as fetal hormone-expressing cells

Graphical abstract

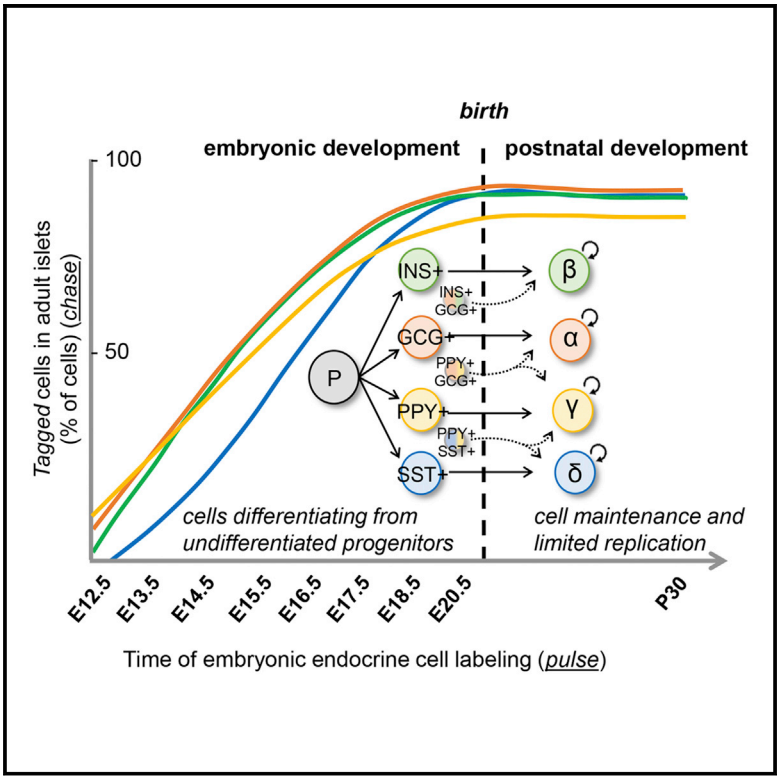

Highlights

- Adult pancreatic islet endocrine cells arise as embryonic hormone-expressing cells
- No detectable islet cell differentiation from putative precursor cells after birth
- Some embryonic hormone-producing cells display a switch in hormone gene expression

Authors

Marta Perez-Frances, Maria Valentina Abate, Delphine Baronnier, Philipp E. Scherer, Yoshio Fujitani, Fabrizio Thorel, Pedro L. Herrera

Correspondence

pedro.herrera@unige.ch

In brief

Perez-Frances et al. describe the natural history of islet endocrine cells in adult and aged (10-month-old) mice, tracing them back to an embryonic origin exclusively. All islet cells emerge from hormone-expressing cells arising already in early pancreatic primordia, with precise patterns of hormone gene activation, co-expression, and switching during development.

Perez-Frances et al., 2022, Cell Reports *38*, 110377
February 15, 2022
https://doi.org/10.1016/j.celrep.2022.110377

CellPress

Cell Reports

CellPress
OPEN ACCESS

Article

Adult pancreatic islet endocrine cells emerge as fetal hormone-expressing cells

Marta Perez-Frances,[1,4] Maria Valentina Abate,[1,4] Delphine Baronnier,[1,4] Philipp E. Scherer,[2] Yoshio Fujitani,[3] Fabrizio Thorel,[1] and Pedro L. Herrera[1,5,*]

[1]Department of Genetic Medicine & Development, iGE3 and Centre Facultaire du Diabète, Faculty of Medicine, University of Geneva, 1211 Geneva, Switzerland

[2]Touchstone Diabetes Center, Departments of Internal Medicine and Cell Biology, The University of Texas Southwestern Medical Center, 5323 Harry Hines Boulevard, Dallas, TX 75390-8549, USA

[3]Laboratory of Developmental Biology & Metabolism, Institute for Molecular & Cellular Regulation, Gunma University, 3-39-15 Showa-machi, Maebashi, Gunma, 371-8512, Japan

[4]These authors contributed equally

[5]Lead contact

*Correspondence: pedro.herrera@unige.ch

https://doi.org/10.1016/j.celrep.2022.110377

SUMMARY

The precise developmental dynamics of the pancreatic islet endocrine cell types, and their interrelation, are unknown. Some authors claim the persistence of islet cell differentiation from precursor cells after birth ("neogenesis"). Here, using four conditional cell lineage tracing ("pulse-and-chase") murine models, we describe the natural history of pancreatic islet cells, once they express a hormone gene, until late in life. Concerning the contribution of early-appearing embryonic hormone-expressing cells to the formation of islets, we report that adult islet cells emerge from embryonic hormone-expressing cells arising at different time points during development, without any evidence of postnatal neogenesis. We observe specific patterns of hormone gene activation and switching during islet morphogenesis, revealing that, within each cell type, cells have heterogeneous developmental trajectories. This likely applies to most maturating cells in the body, and explains the observed phenotypic variability within differentiated cell types. Such knowledge should help devising novel regenerative therapies.

INTRODUCTION

In adult mice, the pancreatic islets contain four main types of cells, named β (producing insulin -Ins), α (glucagon -Gcg), δ (somatostatin -Sst), and γ (pancreatic polypeptide -Ppy). Their combined task is to ensure blood glucose homeostasis. Defects in islet cell function lead to glycemia dysregulation, frequently hyperglycemia and diabetes (Ashcroft and Rorsman, 2012).

Endocrine pancreas ontogeny in rodents was described to encompass two main periods, called "transitions" (R. Pictet, 1972). The pancreas develops from two endodermal primordia in the hepatic-pancreatic ring of the anterior intestinal portal, which is the opening of the primitive foregut into the midgut. The dorsal bud appears at the 29-somite stage (corresponding to 9.5 days of gestation, E9.5, in mouse embryos), whereas the ventral bud, which is the third diverticulum of the hepato-biliary primordium, grows slightly later. The first transition (from E9.5 to E12.5) is a period of active expansion of multipotent progenitors and morphogenesis (epithelial branching) with limited endocrine cell differentiation (Benitez et al., 2012). During the secondary transition (from E13.5 to term) there is a peak of emerging Neurog3-expressing endocrine unipotent precursor cells (Desgraz and Herrera, 2009) that rapidly differentiate into hormone-expressing cells (Villasenor et al., 2008). These early hormone-expressing cells delaminate from the ductal epithelia, and start to cluster in the interstitia of the developing gland (Herrera et al., 1991). This is the beginning of islet formation. Multiple cellular interactions are required for islet morphogenesis, through vascular endothelial growth factor (VEGF) (Cai et al., 2012; Gittes, 2009; Johansson et al., 2006), Sonic Hedgehog (Hibsher et al., 2016), and Wnt (Landsman et al., 2011) signaling. In mice, the first islet-like cell clusters are seen around birth (Villasenor et al., 2008; Pan and Brissova, 2014; Romer and Sussel, 2015). Neurog3^{+} cells do not proliferate, and every single Neurog3-expressing cell becomes an endocrine cell in the islets of newborn mice (Desgraz and Herrera, 2009). Subsequently, islet cells undergo on average one mitosis during the first 2 months of life, and a second division during the following 10 months, which is an important span in a mouse lifetime (Desgraz and Herrera, 2009).

Previous studies report that postnatal islet cell mass expansion and homeostasis rely exclusively on the maintenance of pre-existing hormone-expressing cells and their low proliferation rates (Dor et al., 2004). This was supported by several studies describing that islet endocrine cell populations are composed of long-lived cells that are maintained by self-duplication, which declines with age (Dor et al., 2004; Xiao et al., 2013; Meier et al., 2008; Kopp et al., 2011; Solar et al., 2009; Nakamura et al., 2011;

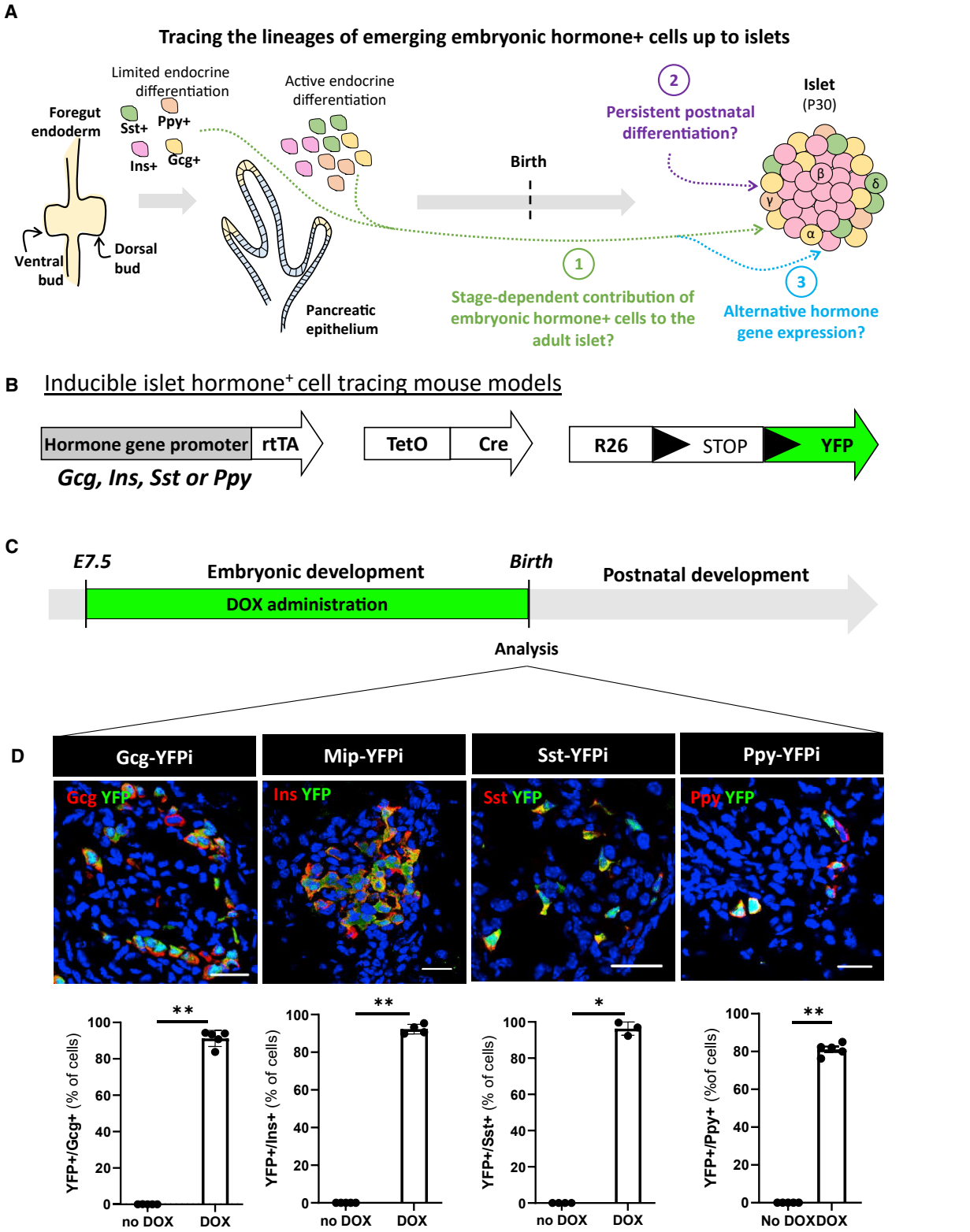

Figure 1. Embryonic hormone-expressing cells become islet endocrine cells

(A) Graphical design of the study aims The first stages of pancreas development (from E9.5 to E12.5) are defined by the formation of two endodermal primordia (the ventral and the dorsal bud), which progressively expand and branch to form the ductal tree. During this period, only a limited endocrine cell differentiation occurs. During the secondary transition (from E13.5 to term), there is a peak of endocrine unipotent precursor cells formation, and a rapid differentiation and

(legend continued on next page)

Kopinke and Murtaugh, 2010; Zhao et al., 2021). Others reported, however, that there is islet β-cell neogenesis from progenitors (mainly ductal cells) after birth (Inada et al., 2008). The cause of this discrepancy is likely due to technical issues inherent to the cell labeling tools used in transgenic mice (i.e., promoter specificity, method of labeling, etc.).

Expression of the transcription factor Neurog3 is a mark of committed unipotent endocrine precursor cells (Gu et al., 2002; Desgraz and Herrera, 2009; Herrera et al., 2002), yet it remains unknown how and when the definitive fate of Neurog3$^+$ cells is established. It was proposed that this terminal differentiation was defined by developmental "competence windows" during pancreas ontogeny (Johansson et al., 2007). The appearance of Gcg- and Ppy-expressing cells was reported as early as E9.5, followed by insulin-producing cells at around E12.5 and lastly somatostatin-producing cells from E13.5 (Herrera et al., 1991), but whether these early hormone-expressing cells become constituents of the adult islets is not known. A great proportion of these early endocrine cells are bihormonal, most of them coexpressing Ppy (Herrera et al., 1991). In fact, embryonic cell ablation and lineage-tracing studies revealed that embryonic *Ppy* expression is required for the differentiation of both adult β- and δ-cells (Herrera et al., 1994; Herrera, 2000), suggesting that embryonic hormone-expressing cells could become adult islet cells expressing different hormones.

Here, we used four DOX-inducible murine lines (two insertional transgenics and two knockin strains) to selectively tag hormone-expressing cells in the pancreas at specific developmental stages, before or after birth, and lineage-trace each islet cell type back to its ontogenetic origin. We describe that all embryonic endocrine cell types, and their progeny, compose the adult islet cell population regardless of their timing of appearance during development. Interestingly, some embryonic hormone-expressing cells can switch hormone gene expression and become a different endocrine cell type in the adult islet. After birth, no evidence of postnatal islet neogenesis from progenitors was observed, for any of the islet cell types, which is compatible with the concept of islet cell homeostasis being ensured by the long lifespan, with low proliferation rates, of the islet endocrine cells present at birth.

RESULTS

DOX-mediated cell labeling traces islet endocrine cells back to their embryonic origin

In this study, we used various experimental designs to (1) investigate the contribution of embryonic hormone-expressing cells to the formation of adult islets, (2) explore whether differentiation of new islet cells from persistent precursors occurs after birth, and (3) determine whether the initiation of hormone gene expression in developing pancreata represents a stable feature of the early endocrine cells that is maintained later in life (Figure 1A). For this purpose, we took advantage of different transgenic mouse models to irreversibly label, following a "pulse-and-chase" approach, embryonic hormone-expressing pancreatic cells (Figure 1B). Embryonic Gcg-, Ins-, Sst-, and Ppy-producing cells were independently labeled and tracked using previously described doxycycline (DOX)-dependent lineage-tracing systems: Gcg-YFPi (Thorel et al., 2010), Sst-YFPi (Cigliola et al., 2018) (knockin), Mip-YFPi (Kusminski et al., 2016), and Ppy-YFPi (Perez-Frances et al., 2021) (knockin). These mice bear three different transgenes: *hormone promoter-rtTA* (glucagon, insulin, somatostatin, or Ppy promoter), *TetO-Cre,* and *R26-YFP* transgenes (Figures 1B and S1).

Because cell labeling efficiency in embryos depends on the efficacy of DOX crossing the placenta, we first evaluated the labeling efficiency in newborns (postnatal day 0, P0) from mothers exposed to DOX during gestation (Figure 1C). While no labeling was detected in the absence of DOX (Figure S1; Gcg-YFPi, n = 5, 0.0% YFP$^+$/Gcg$^+$; Mip-YFPi, n = 4, 0.0% YFP$^+$/Ins$^+$; Sst-YFPi, n = 4, 0.0% YFP$^+$/Sst$^+$; Ppy-YFPi, n = 5, 0.0% YFP$^+$/Ppy$^+$; Source Data table a, b), around 90% of hormone$^+$ cells in neonatal mice were YFP-traced when DOX was administered to pregnant females from 7.5 days post conception (embryonic day E7.5) until term (Figure 1D, Data S1A). Thus, the Gcg-YFPi, Sst-YFPi, Mip-YFPi, and Ppy-YFPi transgenes allow an efficient, inducible, and irreversible labeling of embryonic hormone-producing cells upon DOX administration.

Embryonic hormone-expressing cells form the adult islet cell populations in accordance with specific stage-dependent dynamic developmental patterns

We explored whether embryonic Gcg$^+$, Ins$^+$, Sst$^+$, and Ppy$^+$ cells become adult islet cells. For this purpose, we administered DOX to pregnant females starting from E7.5, so as to cover the entire embryonic period of pancreas development. We then assessed the percentage of hormone$^+$ YFP-labeled cells in young adults (P30, i.e., postnatal day 30, 1 month of age; Figure 2A).

We determined the kinetics of DOX clearance to precisely define the developmental timing of cell labeling (the "pulse" period). For that purpose, we evaluated *Cre* expression, as a proxy of DOX activity, in islets of pregnant Gcg-YFPi, Mip-YFPi, and Sst-YFPi females either during DOX treatment or after

emergence of hormone-expressing cells. These hormone$^+$ cells delaminate from the ductal epithelia to generate clusters in the interstitia. The first islet-like structures are observed after birth.

(B) Transgenes required for tracing the lineages of Gcg-, Ins-, Sst-, and Ppy-expressing cells.

(C) Embryonic Gcg-, Ins-, Sst-, and Ppy-expressing cell labeling strategy. DOX, doxycycline; E7.5, embryonic day 7.5 after conception.

(D) Gcg$^+$, Ins$^+$, Sst$^+$, and Ppy$^+$ cells are efficiently YFP-labeled during embryogenesis. Immunofluorescence of YFP (green)-traced cells coexpressing glucagon (red, left panel), Insulin (red, mid-left panel), Somatostatin (red, mid-right panel), and Ppy (red, right panel) at postnatal day 0 (P0). Scale bars, 20μm. Quantification of the YFP-labeled hormone-expressing cells after birth (P0): 91.2 ± 1.9 (n = 5) of the Gcg$^+$ cells are YFP-traced; 92.3 ± 1.1 (n = 4) of the Ins$^+$ cells are YFP-traced; 96.2 ± 2.1 (n = 3) of the Sst$^+$ cells are YFP-traced and 81.2 ± 1.4 (n = 5) of the Ppy$^+$ cells are YFP-traced. P values: Gcg-YFPi, no DOX vs DOX = 0.0075; Mip-YFPi, no DOX vs DOX = 0.0079; Sst-YFPi, no DOX vs DOX = 0.0286; Ppy-YFPi, no DOX vs DOX = 0.0079. No Gcg$^+$, Ins$^+$, Sst$^+$, and Ppy$^+$ cells were YFP-tagged in absence of DOX. Whole pancreases were collected and analyzed. Data are shown as mean ± SEM. One representative biological replicate of an experiment is presented in the micrographs. Experiments were performed two or more times independently under identical or similar conditions. Quantification details are provided as Data S1A.

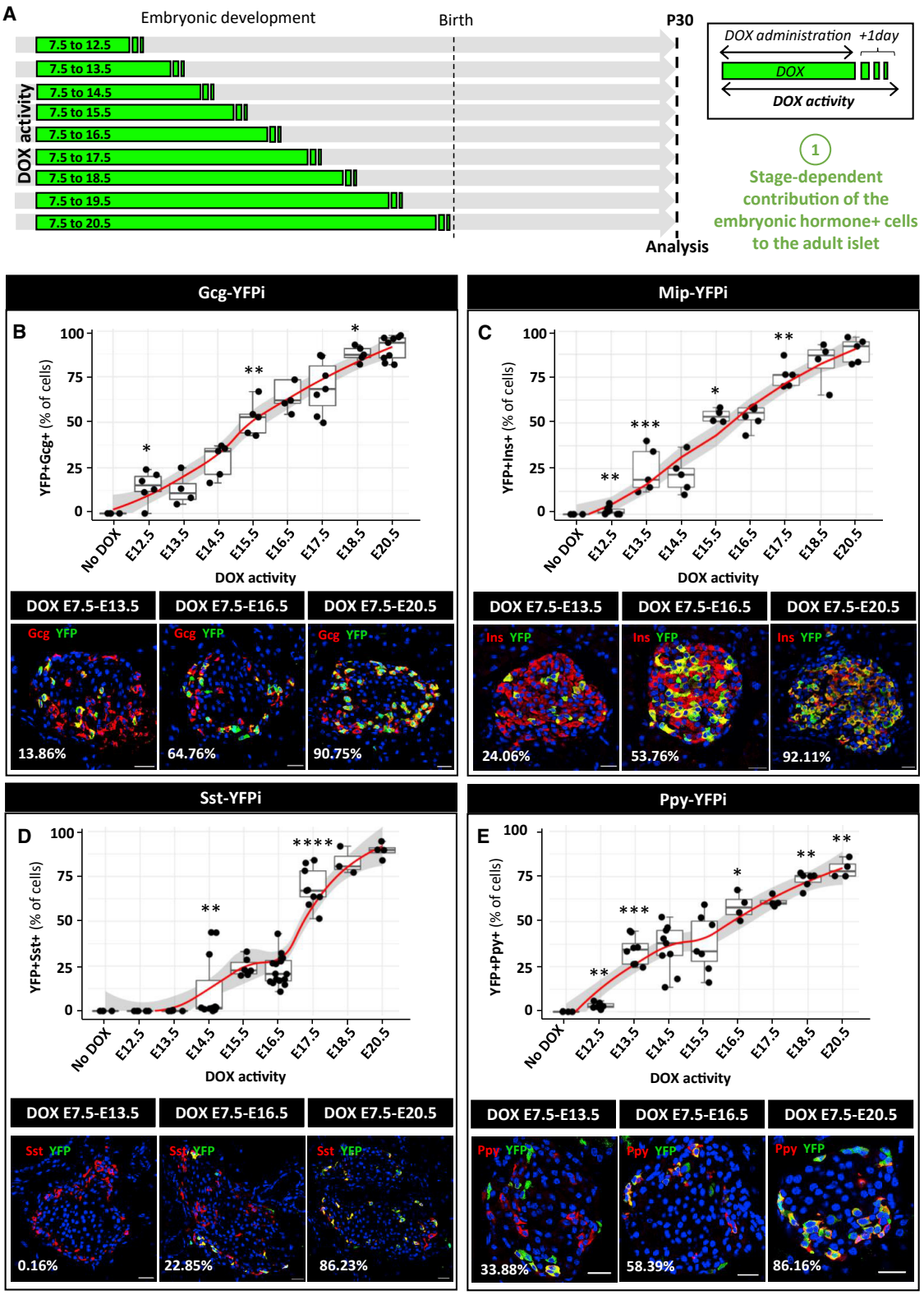

(legend on next page)

DOX withdrawal (Figure S2). As previously shown in Ppy-YFPi mice (Perez-Frances et al., 2021), *Cre* expression sharply decreased to background levels as early as 24 h after DOX withdrawal in all mouse models (Figure S2). Based on this observation, we defined the duration of cell labeling as the period of DOX administration plus 1 additional day (Figure 2A, Data S1C. In subsequent experiments aimed at labeling hormone-expressing cells exclusively during pancreas development, we gave DOX to Gcg-YFPi, Mip-YFPi, Sst-YFPi, and Ppy-YFPi pregnant females from E7.5 until E19.5 (Figure 2A). Incidentally, the four embryonic hormone-expressing cell types were also efficiently labeled after a pulse of 6 to 8 days of DOX administration (Figure S2; Data S1D [Perez-Frances et al., 2021]).

Embryonic GCG$^+$, PPY$^+$, and INS$^+$ cells labeled during the first transition, up to E12.5 (i.e., DOX removed at E11.5 + 1 day of resilient DOX activity) contributed to adult α-, γ -, and β-cell populations to different degrees. The proportion of labeled adult α-cells (14.6% ± 4.3%, n = 6, 573 Gcg$^+$ YFP$^+$ cells out of 4001 Gcg$^+$ cells scored) was higher than that of γ-cells (3.4% ± 0.7%, n = 6, 99 Ppy$^+$ YFP$^+$ cells out of 3223 Ppy$^+$ cells scored) and β-cells (1.8% ± 0.6%, n = 10,355 Ins$^+$ YFP$^+$ cells out of 17,541 Ins$^+$ cells scored). When DOX was given gradually until the end of gestation, the fraction of labeled GCG$^+$, PPY$^+$, and INS$^+$ cells increased accordingly, with similar dynamic progression between cell types (Figures 2B, 2C, and 2E). By contrast, the first embryonic SST$^+$ cells that became adult islet δ-cells appeared at E14.5, at the beginning of the secondary transition (Figure 2D; 11.8% ± 5.5%; n = 11, 388 Sst$^+$ YFP$^+$ cells out of 4,418 Sst$^+$ cells scored). This result confirms that embryonic SST$^+$ cells are the latest hormone-producing cells emerging during pancreas development (Herrera et al., 1991). Also, contrary to the three other hormone-expressing cells, which increase in numbers progressively during development (Figures 2B, 2C, and 2E), SST$^+$ cells giving rise to adult islet δ-cells emerged in two more marked differentiation waves, at E14.5 and E17.5 (Figure 2D). For the four islet cell types, the proportion of labeled cells in adults was maximal when DOX was given until the end of gestation (P0, Figure 1D).

In conclusion, embryonic endocrine cells, and their scarce progeny, whether emerging during the first or secondary transitions, make up the whole adult islet cell populations. Of note, the proportions of labeled adult islet cells observed here when DOX was given for different periods before birth, recapitulate the kinetics of emergence of each embryonic endocrine cell type, being GCG$^+$ and PPY$^+$ cells the first to arise followed by INS$^+$ and then SST$^+$ cells (Herrera et al., 1991).

Islet endocrine cells originate during pancreas ontogeny

We have recently reported that adult γ-cells derive exclusively from Ppy-expressing cells appearing during pancreas development, without detectable postnatal γ-cell differentiation from precursor cells (Perez-Frances et al., 2021). We thus sought to determine if the same applies to the other islet cell types, or a significant fraction of adult α-, β-, and δ-cells arise from postnatal progenitors or precursors (Inada et al., 2008; Nakamura et al., 2011; Kopinke and Murtaugh, 2010; Pan et al., 2013; Dor et al., 2004; Xiao et al., 2013; Meier et al., 2008; Kopp et al., 2011; Solar et al., 2009). We irreversibly labeled embryonic Gcg-, Ins-, and Sst-expressing cells from E7.5 to E20.5, as we did before for γ-cells, and from E7.5 until P30 (Figures 3A and 3B). We then analyzed the percentage of tagged (YFP$^+$) cells in Gcg-YFPi, Mip-YFPi, and Sst-YFPi young and aged adult mice (1 and 10 months of age). If there were *de novo* postnatal differentiation from progenitors/precursors, which would be unlabeled when DOX is given during pancreas development only, then one would expect a lower proportion of labeled adult islet cells in this setting (Figures 3A and 3B).

In young post pubertal mice (1 month old), the proportion of YFP-labeled GCG-, INS-, and SST-producing cells was equivalent regardless of the timing of DOX administration: either before birth (from E7.5 to E20.5) or extended to P30 (from E7.5 to P30; Figures 3C–3E). Interestingly, the percentage of adult YFP-labeled α-, β-, and δ-cells remained stable in aged mice up to 10 months of age as well (Figures 3C–3E). Together, these observations indicate that in normal conditions there is no

Figure 2. Patterns of islet cell emergence during embryonic development

(A) Graphical design of the experiment. Embryonic hormone-expressing cells are labeled from E7.5 for different duration.

(B) Quantification of the YFP-traced Gcg$^+$ cells at postnatal day 30 (P30). No DOX: n = 4, E7.5 to E12.5: n = 6, E7.5 to E13.5: n = 4, E7.5 to E14.5: n = 5, E7.5 to E15.5: n = 5, E7.5 to E16.5: n = 5, E7.5 to E17.5: n = 7, E7.5 to E17.5: n = 5, E7.5 to E20.5: n = 9. p values: No DOX versus E7.5 to E12.5 = 0.0381; E7.5 to E14.5 versus E7.5 to E15.5 = 0.0079; E7.5 to E17.5 versus E7.5 to E18.5 = 0.0303. Representative pictures of the Gcg-expressing YFP-labeled cells when DOX is given from E7.5 to E13.5 (left), to E16.5 (middle), or to E20.5 (right). Red, Gcg; Green, YFP. Scale bars, 20μm.

(C) Quantification of the YFP-traced Ins$^+$ cells at P30. No DOX: n = 4, E7.5 to E12.5: n = 10, E7.5 to E13.5: n = 5, E7.5 to E14.5: n = 5, E7.5 to E15.5: n = 4, E7.5 to E16.5: n = 6, E7.5 to E18.5: n = 4, E7.5 to E20.5: n = 6. p values: No DOX versus E7.5 to E12.5 = 0.009; E7.5 to E12.5 versus E7.5 to E13.5 = 0.001; E7.5 to E14.5 versus E7.5 to E15.5 = 0.0159; E7.5 to E16.5 versus E7.5 to E17.5 = 0.0043. Representative pictures of the Ins-expressing YFP-labeled cells when DOX is given from E7.5 to E13.5 (left), to E16.5 (middle), or to E20.5 (right). Red, Ins; Green, YFP. Scale bars, 20μm.

(D) Quantification of the YFP-traced Sst$^+$ cells at P30. No DOX: n = 4, E7.5 to E12.5: n = 5, E7.5 to E13.5: n = 5, E7.5 to E14.5: n = 11, E7.5 to E15.5: n = 6, E7.5 to E16.5: n = 16, E7.5 to E17.5: n = 9, E7.5 to E18.5: n = 3, E7.5 to E20.5: n = 4. p values: E7.5 to E13.5 versus E7.5 to E14.5 = 0.0034; E7.5 to E16.5 versus E7.5 to E17.5 = 0.0001. Representative pictures of the Sst-expressing YFP-labeled cells when DOX is given from E7.5 to E13.5 (left), to E16.5 (middle), or to E20.5 (right). Red, Sst; Green, YFP. Scale bars, 20μm.

(E) Quantification of the YFP-traced Ppy$^+$ cells at P30. No DOX: n = 4, E7.5 to E12.5: n = 6, E7.5 to E13.5: n = 8, E7.5 to E14.5: n = 9, E7.5 to E16.5: n = 4, E7.5 to E17.5: n = 4, E7.5 to E18.5: n = 6, E7.5 to E20.5: n = 4. p values: no DOX versus E7.5 to E12.5 = 0.0095; E7.5 to 12.5 versus E7.5 to 13.5 = 0.0007; E7.5 to 15.5 versus E7.5 to 16.5 = 0.0424; E7.5 to 17.5 versus E7.5 to 18.5 = 0.0095; E7.5 to 18.5 versus E7.5 to 20.5 = 0.0012. Representative pictures of the Ppy-expressing YFP-labeled cells when DOX is given from E7.5 to E13.5 (left), to E16.5 (middle), or to E20.5 (right). Red, Ppy; Green, YFP. Scale bars, 20μm. Data are shown as mean ± SEM; two-tailed Mann-Whitney test. Gcg$^+$, Sst$^+$, and Ins$^+$ cells were scored in sections from dorsal pancreata, while Ppy$^+$ cells were scored in the ventral pancreas. One representative biological replicate of an experiment is presented in the micrographs. Experiments were performed two or more times independently under identical or similar conditions. Quantification details are provided as Data S1E.

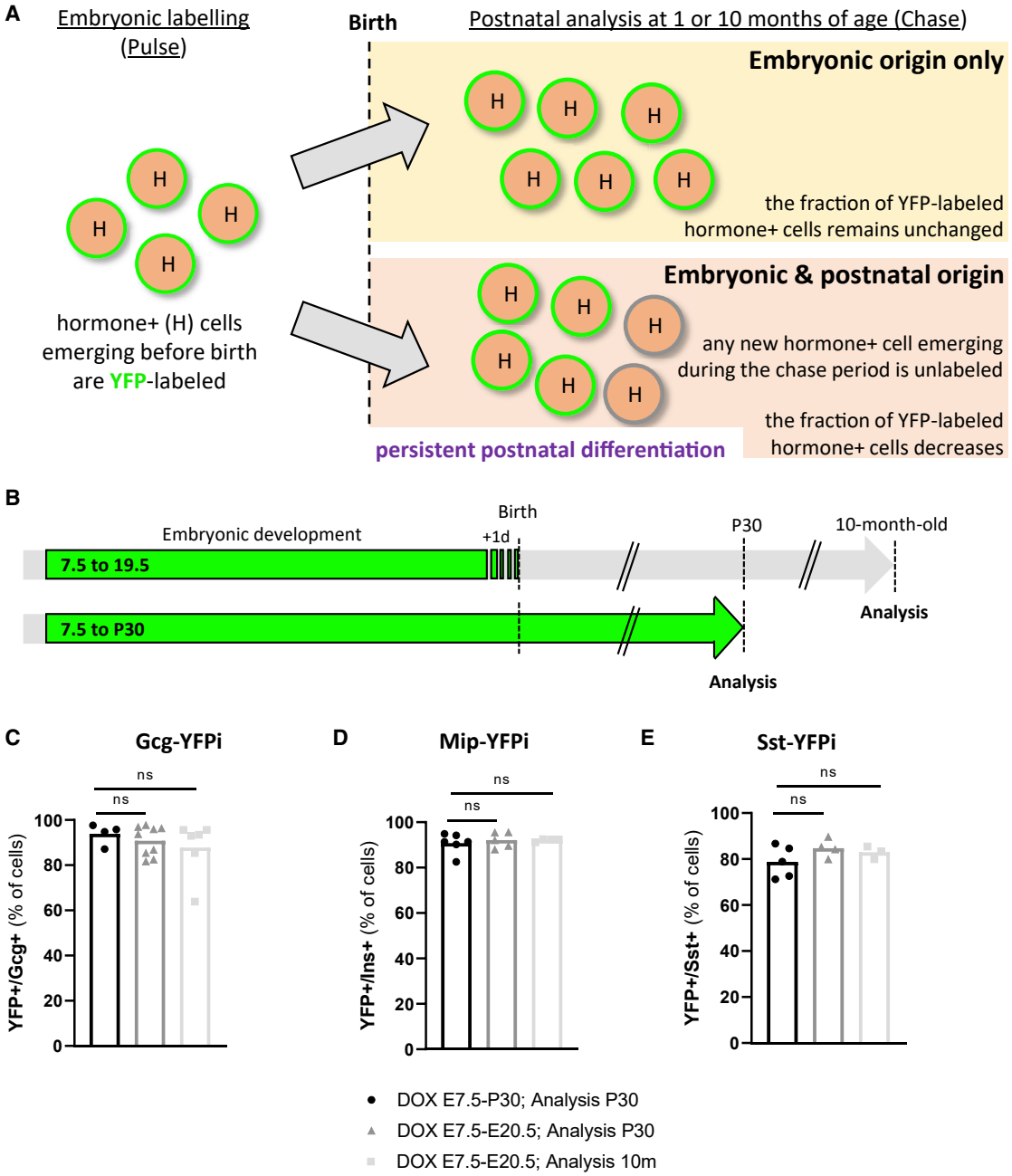

Figure 3. No evidence of postnatal persistence of islet precursor cells

(A) Graphical design of the experimental rationale.

(B) Labeling strategy of embryonic hormone-expressing cells.

(C) The proportion of adult YFP-labeled Gcg-expressing cells is maintained in the different DOX administration periods. DOX E7.5 to P30, analysis P30 (black; n = 4); DOX E7.5 to E20.5, analysis P30 (dark gray, n = 9); DOX E7.5 to E20.5, analysis 10-month-old (light gray, n = 6). p values: DOX E7.5 to P30, analysis P30 versus DOX E7.5 to E20.5, analysis P30 = 0.6042; DOX E7.5 to P30, analysis P30 versus DOX E7.5 to E20.5, analysis long term = 0.271.

(D) The proportion of adult YFP-labeled Ins-expressing cells is maintained in the different DOX administration periods. DOX E7.5 to P30, analysis P30 (black; n = 6); DOX E7.5 to E20.5, analysis P30 (dark gray, n = 5); DOX E7.5 to E20.5, analysis 10-month-old (light gray, n = 4). p values: DOX E7.5 to P30, analysis P30 versus DOX E7.5 to E20.5, analysis P30 = 0.6277; DOX E7.5 to P30, analysis P30 versus DOX E7.5 to E20.5, analysis long term = 0.719.

(E) The proportion of adult YFP-labeled Sst-expressing cells is maintained in the different DOX administration periods. DOX E7.5 to P30, analysis P30 (black; n = 5); DOX E7.5 to E20.5, analysis P30 (dark gray, n = 4); DOX E7.5 to E20.5, analysis 10-month-old (light gray, n = 3). p values: DOX E7.5 to P30, analysis P30 versus DOX E7.5 to E20.5, analysis P30 = 0.2857; DOX E7.5 to P30, analysis P30 versus DOX E7.5 to E20.5, analysis long term = 0.8571. Data are shown as mean ± SEM; two-tailed Mann-Whitney test. Region of the pancreas: Gcg^+ and Ins^+ cells were scored in the dorsal pancreas, Sst^+ and Ppy^+ cells were scored in the ventral pancreas. Experiments were performed two or more times independently under identical or similar conditions. Quantification details are provided as Data S1F.

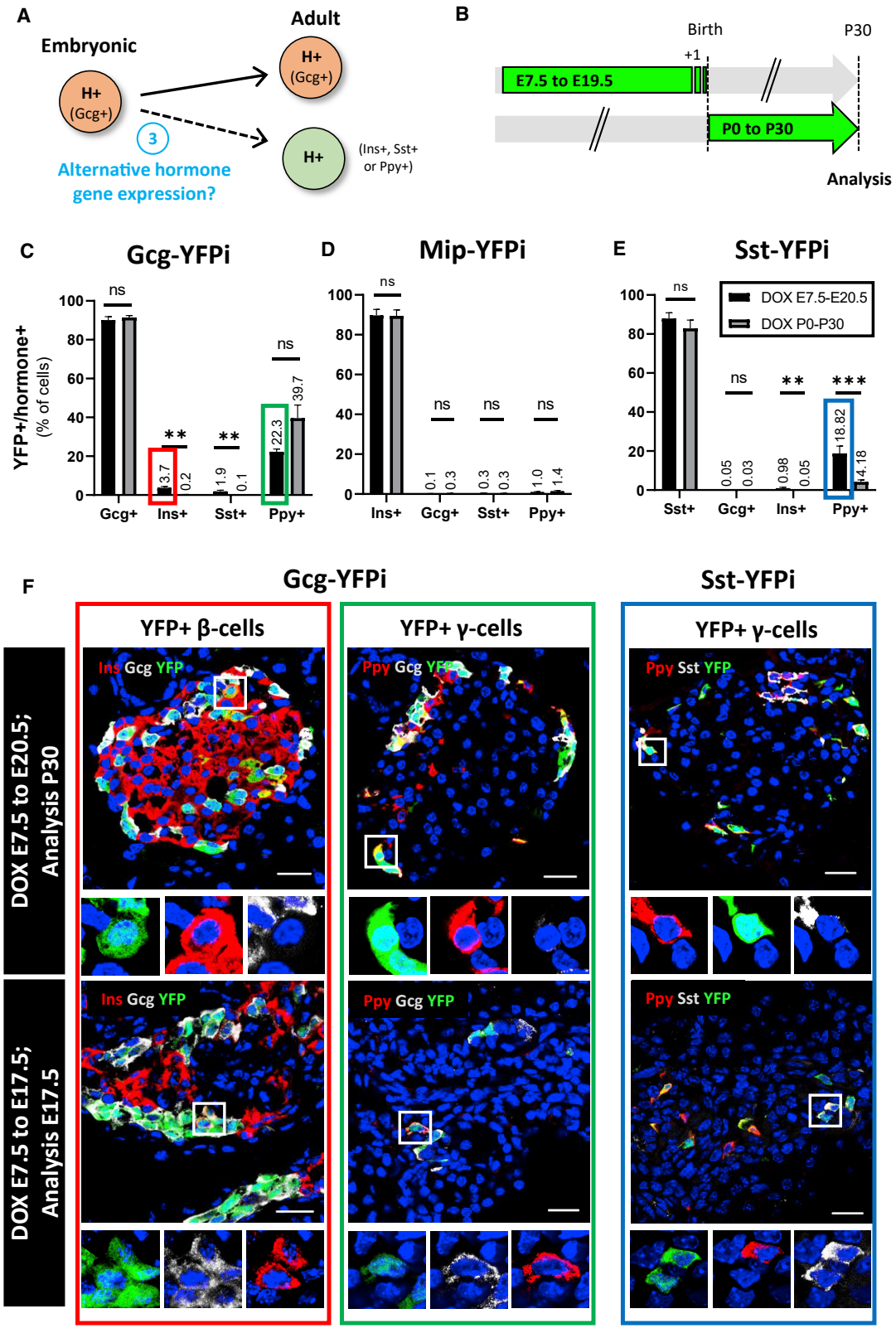

(legend on next page)

detectable postnatal islet cell differentiation from putative undifferentiated progenitor or precursor cells, and suggest that adult α-, β-, and δ-cells emerge from GCG$^+$, INS$^+$, and SST$^+$ cells appearing during pancreas development.

Some embryonic GCG$^+$ and SST$^+$ cells give rise to islet cells that have switched hormone gene expression

Knowing that islet endocrine cells derive from fetal pancreatic hormone-expressing cells, we then aimed at assessing whether embryonic hormone-expressing cells continue expressing the very same hormone gene postnatally, in adult islets (Figure 4A).

We analyzed islets from adult mice in which islet cells had been genetically labeled either during development (from E7.5 to E20.5) or exclusively after birth (DOX from P0 to P30, i.e., from birth to 1 month of age; Figure 4B). We observed that irreversibly labeling embryonic GCG$^+$, INS$^+$, and SST$^+$ cells mainly results in YFP-traced adult α-, β-, and δ-cells, respectively (Figures 4C–4E; Gcg-YFPi: 90.1% of Gcg$^+$ cells were YFP-labeled; Mip-YFPi: 89.7% Ins$^+$ cells were YFP-labeled; Sst-YFPi: 88.0% Sst$^+$ cells were YFP-labeled; Source Data Table G). Similarly, we recently showed that the vast majority of adult γ-cells derive from embryonic Ppy-expressing cells (Perez-Frances et al., 2021). Thus, most pancreatic islet endocrine cells maintain the expression of the very same hormone gene expressed upon differentiation in the pancreatic primordia.

Interestingly, however, about one-fifth of adult Ppy-expressing cells derive from embryonic GCG$^+$ cells and a similar fraction from SST$^+$ cells (Figures 4C and 4E). These γ-cells often maintain Gcg and Sst expression, respectively, and are therefore adult bihormonal Ppy-expressing cells (Figure S3 (Perez-Frances et al., 2021)). This suggests that the adult γ-cell population is heterogeneous, as we recently reported, because these cells derive from different types of embryonic hormone-expressing cells: GCG$^+$, SST$^+$, and PPY$^+$ cells (Figure 4C, 4E, 4F [Perez-Frances et al., 2021]). This notion is supported by the presence of bihormonal PPY$^+$GCG$^+$ and PPY$^+$SST$^+$ cells during embryonic development as well (E17.5; Figure 4F).

Likewise, almost 4% of adult β-cells were YFP-labeled using the Gcg-YFPi mice, indicating that they derived from embryonic cells having expressed Gcg (Figures 4C and 4F). The same fraction of tagged β cells was observed using an independent Gcg-YFPi mouse line, derived from a different founder mouse (not shown). In agreement with this, insulin cells coexpressing glucagon (bihormonal INS$^+$GCG$^+$ cells) have been observed in the fetal pancreas (Figure 4F) (Jeon et al., 2009, Van Gurp et al., 2019). These bihormonal cells were YFP-traced using both Gcg-YFPi and Mip-YFPi (Figures 4F and S3). The fact that there was virtually no α-cell labeled using the Mip-YFPi system (Figure 4D), while 4% β-cells was YFP-traced with Gcg-YFPi (Figure 4C), suggests that bihormonal INS$^+$GCG$^+$ give rise to adult β cells. Of note, embryonic Ins-expressing cells (including the bihormonal INS$^+$GCG$^+$, INS$^+$SST$^+$, and INS$^+$PPY$^+$ cells) only give rise to adult β cells, as virtually no α-, δ-, and γ-cell was labeled using the Mip-YFPi system (Figure 4D). This reveals that insulin gene expression is a terminal differentiation feature.

Altogether, these results suggest that while fetal INS$^+$ cells only become adult β cells, fetal GCG$^+$ cells also give rise to fractions of γ- and β-cells, and some fetal SST$^+$ cells become γ-cells in adult islets.

DISCUSSION

Thanks to the Cre/LoxP system, tracing back the lineages of cells to their embryonic origin (Herrera, 2000) is a powerful approach to explore complex biological processes in fetal and adult tissues, as well as in health and disease. These include organogenesis, tissue differentiation, or cell proliferation and plasticity. Conditional cell labeling enables genetically tagging a given cell population for a specific period (the "pulse"), during development or at any time in postnatal life, and then track its fate subsequently (the "chase"). The first, and most used, inducible Cre was a chimeric Cre fusion protein comprising a tamoxifen (TAM)-specific estrogen receptor (CreER) (Kretzschmar and Watt, 2012). The system is powerful but has limitations, since TAM is an estrogen receptor antagonist. TAM disturbs multiple cellular processes, including embryo development and viability (Patel et al., 2017; Donocoff et al., 2020), and its clearance is slow, which prevents its use in pulse-chase experiments requiring short and precise pulses, i.e., a controlled and rapidly ending Cre activity (Reinert et al., 2012). Contrariwise, DOX-dependent Cre activity is rapid and efficient (>90%), and residual Cre activity only lasts for 1 day after DOX withdrawal, thus making the Tet-ON system ideal for short pulses.

Figure 4. Embryonic hormone-expressing cells have variable fates in adult islets

(A) Cartoon depicting the experimental rationale.

(B) Strategy for labeling embryonic hormone-expressing cells.

(C) Proportion of adult hormone-expressing cells labeled with YFP using the Gcg-YFPi tracing system. p values: Ins$^+$ cells (E7.5 to E20.5 versus P0 to P30) = 0.0025; Sst$^+$ cells (E7.5 to E20.5 versus P0 to P30) = 0.0016.

(D) Proportion of adult hormone-expressing cells labeled with YFP using the Mip-YFPi tracing system. p values: Gcg$^+$ cells (E7.5 to E20.5 versus P0 to P30) = 0.1558; Ins$^+$ cells (E7.5 to E20.5 versus P0 to P30) = 0.9307; Sst$^+$ cells (E7.5 to E20.5 versus P0 to P30) = 0.9134; Ppy+ cells (E7.5 to E20.5 versus P0 to P30) = 0.2251.

(E) Proportion of adult hormone-expressing cells labeled with YFP using the Sst-YFPi tracing system. p values: Ins$^+$ cells (E7.5 to E20.5 versus P0 to P30) = 0.0079; Ppy$^+$ cells (E7.5 to E20.5 versus P0 to P30) = 0.001. Data are shown as mean ± SEM; two-tailed Mann-Whitney test.

(F) Immunofluorescence of adult YFP-labeled Ins- (top left, red rectangle; Ins, red; YFP, green; Gcg, gray) and Ppy- (top middle, green rectangle; Ppy, red; YFP, green; Gcg, gray) expressing cells after DOX administration during the embryonic period using the Gcg-YFPi system. Using the Sst-YFPi system, some adult Ppy-expressing cells are YFP-labeled (top right, blue rectangle; Ppy, red; YFP, green; Sst, gray). Bihormonal YFP-labeled Ins$^+$ Gcg$^+$ (bottom left; Ins, red; YFP, green; Gcg, gray), Gcg$^+$ Ppy$^+$ (bottom middle; Ppy, red; YFP, green; Gcg, gray) and Sst$^+$ Ppy$^+$ (bottom right; Ppy, red; YFP, green; Sst, gray) cells were detected at E17.5. Scale bars, 20μm (10μm in insets). One representative biological replicate of an experiment is presented in the micrographs. Experiments were performed two or more times independently under identical or similar conditions. Quantification details are provided as Data S1G.

Here, we noticed that cell YFP-labeling efficiency in Ppy-YFPi mice was slightly lower (81.2%) than in the other mouse lines (>90%; Figure 1D). We speculate that this difference could be because PPY$^+$ cells are often bihormonal in embryos (Herrera et al., 1994). Yet, we have observed that bihormonal PPY-expressing cells have less *Ppy* expression than monohormonal PPY$^+$ cells in adult islets (Figure S3D) (Perez-Frances et al., 2021). Lower *Ppy* expression in bihormonal cells would lead to lower *rtTA* and *Cre* expression levels, and thus to lower labeling efficiency (Perez-Frances et al., 2021).

Using the DOX system, we report that all the adult islet cell populations originate from embryonic hormone-expressing cells appearing mostly after the secondary transition. Concerning α-cells, two-thirds of them originate from embryonic glucagon-expressing cells emerging before E14.5. This is in line with previous reports showing that glucagon$^+$ cells are one of the first endocrine cells appearing during pancreas development (Herrera et al., 1991). Yet Johansson and colleagues described that the competence of pancreatic epithelial cells to produce glucagon was dramatically decreased after E14.5 (Johansson et al., 2007). This discrepancy could be explained because of the forced ectopic expression of *Neurog3* in all endodermal epithelial cells of pancreatic primordia.

Overall, we did not observe any specific competence window for the embryonic endocrine cells to constitute the adult α-, β-, and γ-cell populations. Instead, a constant and progressive contribution of embryonic GCG$^+$, INS$^+$, and PPY$^+$ cells was observed. The kinetics of embryonic somatostatin-expressing cells was different, however, for they appeared in two bursts occurring during the secondary transition (Figure 3D). The late origin of the adult δ-cell population during pancreas organogenesis was already reported (Herrera et al., 1991; Argenton et al., 1999).

The mechanism of adult islet cell maintenance, particularly for β cells, is still a matter of debate. While this article was under evaluation, Gribben et al. (2021) reported the presence of Neurog3$^+$ cells in pancreatic ducts that co-express somatostatin and insulin and suggest that these cells maintain the adult islet β-cell population. Yet, several concerns remain in this and in previous studies, such as promoter specificity (Hnf1β-CreER and Neurog3-CreER transgenes directly label δ-cells) and TAM clearance. In the present study, using carefully controlled transgenes, two of which were knockins, we could not gather evidence supporting the very existence of such an adult islet stem cell. Even if cell labeling efficiency is never 100%, if there were a small percentage of islet cells differentiated in postnatal life, one would expect some variation in the numbers of tagged cells after 10 months. Yet the percentage of labeled islet cells always remained maximal and identical to the maximum efficiency of recombination. Thus, our observations are compatible with the notion that islet maintenance during life relies on the longevity with low proliferation rates of the endocrine cells present at birth (Perez-Frances et al., 2021). Under injury or metabolic stress, regenerative processes involving alternative sources, such as islet non-β-cell-type interconversion, may become relevant (Cigliola et al., 2018, 2020; Chera et al., 2014; Thorel et al., 2010; Ye et al., 2016; Bernard-Kargar and Ktorza, 2001; Zhao et al., 2021).

Classic studies confirmed by more recent work indicate that adult islet cells, especially β cells, have heterogeneous profiles and functionality (Dominguez-Gutierrez et al., 2019; Montefusco et al., 2020; Roscioni et al., 2016; Baron et al., 2016; Avrahami et al., 2017). We have recently reported that adult γ-cells are also heterogeneous, with different kinds of bihormonal expression, both in mice and men (Perez-Frances et al., 2021). Although the molecular signature of these adult subpopulations has been well characterized at the mRNA level (single-cell sequencing), the origin and meaning of this cell heterogeneity remains enigmatic. Here, we report that around 4% of the β cells derive from embryonic glucagon-expressing cells. This means that some of the fetal glucagon-expressing cells cease glucagon expression to become insulin expressers. This contradicts the assumption that the early human GCG$^+$ INS$^+$ bihormonal cells become adult α cells (Riedel et al., 2012), which was proposed based on transcription factor coexpression patterns. Yet marker colocalization alone is not evidence of a common ontogeny/ancestry (i.e., same lineage). Interestingly, and on the contrary, the embryonic cells that engage *Ins* gene expression do not change to activate the expression of any other hormone gene, indicating that *Ins* gene expression represents a terminal differentiation event.

We also report that a fraction of adult PPY$^+$ cells derives from cells that express Gcg or Sst during embryonic life. Likewise, a fraction of adult α and δ cells originates from cells that expressed Sst and Gcg before birth, respectively. The presence of bihormonal PPY$^+$ GCG$^+$ and PPY$^+$ SST$^+$ cells in adult islets (Perez-Frances et al., 2021) suggests that they acquired hormone coexpression during fetal life and some of them maintain it postnatally. Thus, it appears that heterogeneity within individual islet cell types has a developmental origin. Whether these differences in ancestry result in peculiar cell functions or regenerative capacities in islet cells remains to be elucidated. Combination of conditional cell lineage-tracing studies and single-cell transcriptomics should help determine the relevance of the developmental and phenotypic heterogeneity in adult islet cell function.

Defining the precise developmental origin of adult cells provides fundamental information for understanding the basis of cell heterogeneity. This variability in turn determines the making of the organs, like the islets, and thus the pathogeny of disease. The varying and somewhat unfixed embryonic origins of mature and differentiated cell populations, likely dictates the observed intrinsic variability in cell identity, function, and plasticity potential. Such knowledge should help developing innovative strategies in regenerative medicine, like finding ways to potentiate the Gcg-to-Ins switch, naturally occurring in the developing pancreas, as shown herein, and after massive β cell loss (Thorel et al., 2010), to treat diabetes.

Limitations of the study

We have shown that the adult islet cell populations originate from embryonic endocrine cells, and found no evidence of postnatal islet cell differentiation from putative undifferentiated precursor cells. In any experimental research, all conclusions are based on probabilities. Here, cell labeling rates in embryos and adults never reached the 100% value. This is an intrinsic limitation. However, our data clearly suggest that, if anything, only an undetectable negligible fraction of islet endocrine cells would originate postnatally from progenitors in physiological conditions.

We have observed that some embryonic endocrine cells can change hormone gene expression during pancreas development and give rise to adult islet cells expressing a different hormone gene. We propose that these patterns of hormone gene switch occur through transient bihormonal states during embryonic stages. Such bihormonal cells are abundant in pancreatic primordia, yet to formally prove that they actually are these intermediates, new genetic tools labeling specifically bihormonal cells would be required.

STAR★METHODS

Detailed methods are provided in the online version of this paper and include the following:

- KEY RESOURCES TABLE
- RESOURCE AVAILABILITY
  - Lead contact
  - Material availability
  - Data and code availability
- EXPERIMENTAL MODEL AND SUBJECT DETAILS
  - Animal models
- METHOD DETAILS
  - Doxycycline
  - Islet isolation and RNA extraction
  - RT-qPCR
  - Immunofluorescence
- QUANTIFICATION AND STATISTICAL ANALYSIS

SUPPLEMENTAL INFORMATION

Supplemental information can be found online at https://doi.org/10.1016/j.celrep.2022.110377.

ACKNOWLEDGMENTS

We thank B. Polat, G. Gallardo, and O. Fazio for technical help, and Drs A. Grapin-Botton, S. Chera, L. Ghila, D. Oropeza, E. Bru-Tari, and L. van Gurp for carefully reading the manuscript. This work was funded with grants from the Swiss National Science Foundation (#310030_192496), the Fondation Aclon 2019-21, and the European Research Council ("Merlin" project, #884449) to P.L.H.

AUTHOR CONTRIBUTION

M.P.F., M.V.A., and D.B. conceived and performed the experiments and analyses; M.P.F. wrote the manuscript; P.E.S. provided the Mip-rtTA transgene; Y.F. generated and provided the PPY antibody; F.T. and P.L.H. generated the Gcg-rtTA, Sst-rtTA, and Ppy-rtTA mouse line, conceived the experiments, interpreted the observations, and wrote the manuscript.

DECLARATION OF INTERESTS

The authors declare no competing interests.

Received: September 21, 2021
Revised: December 7, 2021
Accepted: January 21, 2022
Published: February 15, 2022

REFERENCES

Argenton, F., Zecchin, E., and Bortolussi, M. (1999). Early appearance of pancreatic hormone-expressing cells in the zebrafish embryo. Mech. Dev. *87*, 217–221.

Ashcroft, F.M., and Rorsman, P. (2012). Diabetes mellitus and the β cell: the last ten years. Cell *148*, 1160–1171.

Avrahami, D., Wang, Y.J., Klochendler, A., Dor, Y., Glaser, B., and Kaestner, K.H. (2017). β-Cells are not uniform after all-Novel insights into molecular heterogeneity of insulin-secreting cells. Diabetes Obes. Metab. *19*, 147–152.

Baron, M., Veres, A., Wolock, S.L., Faust, A.L., Gaujoux, R., Vetere, A., Ryu, J.H., Wagner, B.K., Shen-Orr, S.S., Klein, A.M., et al. (2016). A single-cell transcriptomic map of the human and mouse pancreas reveals inter- and intra-cell population structure. Cell Syst. *3*, 346–360.e4.

Benitez, C.M., Goodyer, W.R., and Kim, S.K. (2012). Deconstructing pancreas developmental biology. Cold Spring Harb Perspect. Biol. *4*, a012401.

Bernard-Kargar, C., and Ktorza, A. (2001). Endocrine pancreas plasticity under physiological and pathological conditions. Diabetes *50*, S30–S35.

Cai, Q., Brissova, M., Reinert, R.B., Pan, F.C., Brahmachary, P., Jeansson, M., Shostak, A., Radhika, A., Poffenberger, G., Quaggin, S.E., et al. (2012). Enhanced expression of VEGF-A in β cells increases endothelial cell number but impairs islet morphogenesis and β cell proliferation. Dev. Biol. *367*, 40–54.

Chera, S., Baronnier, D., Ghila, L., Cigliola, V., Jensen, J.N., Gu, G., Furuyama, K., Thorel, F., Gribble, F.M., Reimann, F., and Herrera, P.L. (2014). Diabetes recovery by age-dependent conversion of pancreatic δ-cells into insulin producers. Nature *514*, 503–507.

Cigliola, V., Ghila, L., Chera, S., and Herrera, P.L. (2020). Tissue repair brakes: a common paradigm in the biology of regeneration. Stem Cells *38*, 330–339.

Cigliola, V., Ghila, L., Thorel, F., Van Gurp, L., Baronnier, D., Oropeza, D., Gupta, S., Miyatsuka, T., Kaneto, H., Magnuson, M.A., et al. (2018). Pancreatic islet-autonomous insulin and smoothened-mediated signalling modulate identity changes of glucagon(+) α-cells. Nat. Cell Biol. *20*, 1267–1277.

Desgraz, R., and Herrera, P.L. (2009). Pancreatic neurogenin 3-expressing cells are unipotent islet precursors. Development *136*, 3567–3574.

Dominguez-Gutierrez, G., Xin, Y., and Gromada, J. (2019). Heterogeneity of human pancreatic β-cells. Mol. Metab. *27s*, S7–S14.

Donocoff, R.S., Teteloshvili, N., Chung, H., Shoulson, R., and Creusot, R.J. (2020). Optimization of tamoxifen-induced Cre activity and its effect on immune cell populations. Sci. Rep. *10*, 15244.

Dor, Y., Brown, J., Martinez, O.I., and Melton, D.A. (2004). Adult pancreatic beta-cells are formed by self-duplication rather than stem-cell differentiation. Nature *429*, 41–46.

Gittes, G.K. (2009). Developmental biology of the pancreas: a comprehensive review. Dev. Biol. *326*, 4–35.

Gribben, C., Lambert, C., Messal, H.A., Hubber, E.L., Rackham, C., Evans, I., Heimberg, H., Jones, P., Sancho, R., and Behrens, A. (2021). Ductal Ngn3-expressing progenitors contribute to adult β cell neogenesis in the pancreas. Cell Stem Cell *28*, 2000–2008.e4.

Gu, G., Dubauskaite, J., and Melton, D.A. (2002). Direct evidence for the pancreatic lineage: NGN3+ cells are islet progenitors and are distinct from duct progenitors. Development *129*, 2447–2457.

Herrera, P.L. (2000). Adult insulin- and glucagon-producing cells differentiate from two independent cell lineages. Development *127*, 2317–2322.

Herrera, P.L., Huarte, J., Sanvito, F., Meda, P., Orci, L., and Vassalli, J.D. (1991). Embryogenesis of the murine endocrine pancreas; early expression of pancreatic polypeptide gene. Development *113*, 1257–1265.

Herrera, P.L., Huarte, J., Zufferey, R., Nichols, A., Mermillod, B., Philippe, J., Muniesa, P., Sanvito, F., Orci, L., and Vassalli, J.D. (1994). Ablation of islet endocrine cells by targeted expression of hormone-promoter-driven toxigenes. Proc. Natl. Acad. Sci. U S A. *91*, 12999–13003.

Herrera, P.L., Nepote, V., and Delacour, A. (2002). Pancreatic cell lineage analyses in mice. Endocrine *19*, 267–278.

Hibsher, D., Epshtein, A., Oren, N., and Landsman, L. (2016). Pancreatic mesenchyme regulates islet cellular composition in a patched/hedgehog-dependent manner. Sci. Rep. *6*, 38008.

Inada, A., Nienaber, C., Katsuta, H., Fujitani, Y., Levine, J., Morita, R., Sharma, A., and Bonner-Weir, S. (2008). Carbonic anhydrase II-positive pancreatic cells are progenitors for both endocrine and exocrine pancreas after birth. Proc. Natl. Acad. Sci. U S A. *105*, 19915–19919.

Jeon, J., Correa-Medina, M., Ricordi, C., Edlund, H., and Diez, J.A. (2009). Endocrine cell clustering during human pancreas development. J. Histochem. Cytochem. *57*, 811–824.

Johansson, K.A., Dursun, U., Jordan, N., Gu, G., Beermann, F., Gradwohl, G., and Grapin-Botton, A. (2007). Temporal control of neurogenin3 activity in pancreas progenitors reveals competence windows for the generation of different endocrine cell types. Dev. Cell *12*, 457–465.

Johansson, M., Andersson, A., Carlsson, P.O., and Jansson, L. (2006). Perinatal development of the pancreatic islet microvasculature in rats. J. Anat. *208*, 191–196.

Kopinke, D., and Murtaugh, L.C. (2010). Exocrine-to-endocrine differentiation is detectable only prior to birth in the uninjured mouse pancreas. BMC Dev. Biol. *10*, 38.

Kopp, J.L., Dubois, C.L., Schaffer, A.E., Hao, E., Shih, H.P., Seymour, P.A., Ma, J., and Sander, M. (2011). Sox9+ ductal cells are multipotent progenitors throughout development but do not produce new endocrine cells in the normal or injured adult pancreas. Development *138*, 653–665.

Kretzschmar, K., and Watt, F.M. (2012). Lineage tracing. Cell *148*, 33–45.

Kusminski, C.M., Chen, S., Ye, R., Sun, K., Wang, Q.A., Spurgin, S.B., Sanders, P.E., Brozinick, J.T., Geldenhuys, W.J., Li, W.H., et al. (2016). MitoNEET-parkin effects in pancreatic α- and β-cells, cellular survival, and intrainsular cross talk. Diabetes *65*, 1534–1555.

Landsman, L., Nijagal, A., Whitchurch, T.J., Vanderlaan, R.L., Zimmer, W.E., Mackenzie, T.C., and Hebrok, M. (2011). Pancreatic mesenchyme regulates epithelial organogenesis throughout development. Plos Biol. *9*, e1001143.

Meier, J.J., Butler, A.E., Saisho, Y., Monchamp, T., Galasso, R., Bhushan, A., Rizza, R.A., and Butler, P.C. (2008). Beta-cell replication is the primary mechanism subserving the postnatal expansion of beta-cell mass in humans. Diabetes *57*, 1584–1594.

Montefusco, F., Cortese, G., and Pedersen, M.G. (2020). Heterogeneous alpha-cell population modeling of glucose-induced inhibition of electrical activity. J. Theor. Biol. *485*, 110036.

Nakamura, K., Minami, K., Tamura, K., Iemoto, K., Miki, T., and Seino, S. (2011). Pancreatic β-cells are generated by neogenesis from non-β-cells after birth. Biomed. Res. *32*, 167–174.

Pan, F.C., Bankaitis, E.D., Boyer, D., Xu, X., Van De Casteele, M., Magnuson, M.A., Heimberg, H., and Wright, C.V. (2013). Spatiotemporal patterns of multipotentiality in Ptf1a-expressing cells during pancreas organogenesis and injury-induced facultative restoration. Development *140*, 751–764.

Pan, F.C., and Brissova, M. (2014). Pancreas development in humans. Curr. Opin. Endocrinol. Diabetes Obes. *21*, 77–82.

Patel, S.H., O'hara, L., Atanassova, N., Smith, S.E., Curley, M.K., Rebourcet, D., Darbey, A.L., Gannon, A.L., Sharpe, R.M., and Smith, L.B. (2017). Low-dose tamoxifen treatment in juvenile males has long-term adverse effects on the reproductive system: implications for inducible transgenics. Sci. Rep. *7*, 8991.

Perez-Frances, M., Van Gurp, L., Abate, M.V., Cigliola, V., Furuyama, K., Brutari, E., Oropeza, D., Carreaux, T., Fujitani, Y., Thorel, F., and Herrera, P.L. (2021). Pancreatic Ppy-expressing γ-cells display mixed phenotypic traits and the adaptive plasticity to engage insulin production. Nat. Commun. *12*, 4458.

R. Pictet, W.J.R. (1972). Development of the embryonic endocrine pancreas. The Endocrine Pancreas, *Vol 1* (Washington: American Physiological Society), Section 8.

Reinert, R.B., Kantz, J., Misfeldt, A.A., Poffenberger, G., Gannon, M., Brissova, M., and Powers, A.C. (2012). Tamoxifen-Induced cre-loxP recombination is prolonged in pancreatic islets of adult mice. PLoS One *7*, e33529.

Riedel, M.J., Asadi, A., Wang, R., Ao, Z., Warnock, G.L., and Kieffer, T.J. (2012). Immunohistochemical characterisation of cells co-producing insulin and glucagon in the developing human pancreas. Diabetologia *55*, 372–381.

Romer, A.I., and Sussel, L. (2015). Pancreatic islet cell development and regeneration. Curr. Opin. Endocrinol. Diabetes Obes. *22*, 255–264.

Roscioni, S.S., Migliorini, A., Gegg, M., and Lickert, H. (2016). Impact of islet architecture on β-cell heterogeneity, plasticity and function. Nat. Rev. Endocrinol. *12*, 695–709.

Solar, M., Cardalda, C., Houbracken, I., Martín, M., Maestro, M.A., De Medts, N., Xu, X., Grau, V., Heimberg, H., Bouwens, L., and Ferrer, J. (2009). Pancreatic exocrine duct cells give rise to insulin-producing beta cells during embryogenesis but not after birth. Dev. Cell *17*, 849–860.

Thorel, F., Népote, V., Avril, I., Kohno, K., Desgraz, R., Chera, S., and Herrera, P.L. (2010). Conversion of adult pancreatic alpha-cells to beta-cells after extreme beta-cell loss. Nature *464*, 1149–1154.

Van Gurp, L., Muraro, M.J., Dielen, T., Seneby, L., Dharmadhikari, G., Gradwohl, G., Van Oudenaarden, A., and De Koning, E.J.P. (2019). A transcriptomic roadmap to α- and β-cell differentiation in the embryonic pancreas. Development *146*. https://doi.org/10.1242/dev.173716.

Villasenor, A., Chong, D.C., and Cleaver, O. (2008). Biphasic Ngn3 expression in the developing pancreas. Dev. Dyn. *237*, 3270–3279.

Xiao, X., Chen, Z., Shiota, C., Prasadan, K., Guo, P., El-Gohary, Y., Paredes, J., Welsh, C., Wiersch, J., and Gittes, G.K. (2013). No evidence for β cell neogenesis in murine adult pancreas. J. Clin. Invest *123*, 2207–2217.

Ye, R., Wang, M., Wang, Q.A., Spurgin, S.B., Wang, Z.V., Sun, K., and Scherer, P.E. (2016). Autonomous interconversion between adult pancreatic α-cells and β-cells after differential metabolic challenges. Mol. Metab. *5*, 437–448.

Zhao, H., Huang, X., Liu, Z., Pu, W., Lv, Z., He, L., Li, Y., Zhou, Q., Lui, K.O., and Zhou, B. (2021). Pre-existing beta cells but not progenitors contribute to new beta cells in the adult pancreas. Nat. Metab. *3*, 352–365.

STAR★METHODS

KEY RESOURCES TABLE

REAGENT or RESOURCE	SOURCE	IDENTIFIER
Antibodies		
Rabbit anti-insulin	Molecular Probes	Cat# 701265; RRID :AB_2532448
Mouse anti-glucagon	Sigma	Cat# G2654; RRID: AB_259852
rabbit anti-somatostatin	DAKO	Cat# A0566; RRID: AB_2688022
mouse anti-Ppy (clone 23-2D3)	IBL	Cat# 10501
rabbit anti-GFP	Molecular Probes	Cat# A11122; RRID: AB_221569
Chemicals, peptides, and recombinant proteins		
Doxycycline (1 mg/ml)	Sigma	Catalog # D9891
PowerUp^{TM} SYBR^{TM} Green Master Mix	ThermoFisher	Catalog # A25742
Histopaque-1119	Sigma	Catalog # 11191
Collagenase IV	Sigma	Catalog # C7657
guinea pig anti-porcine insulin (1/400)	Dako	Cat# A0564; RRID: AB_10013624
rabbit anti-insulin (1/3000)	Molecular Probes	Cat# 701265; RRID :AB_2532448
mouse anti-glucagon (1/1000)	Sigma	Cat# G2654; RRID: AB_259852
rabbit anti-glucagon (1/200)	Dako	Cat# A0565; RRID: AB_10013726
mouse anti-somatostatin (1/200)	BCBC	Cat# Ab1985; RRID: AB_10014609
rabbit anti-somatostatin (1/200)	Dako	Cat# A0566; RRID: AB_2688022
goat anti-somatostatin (1/200)	Santa Cruz Biotechnology	Cat# sc-55565; RRID: AB_831726 (out of stock)
rabbit anti-GFP (1/400)	Molecular Probes	Cat# A11122; RRID: AB_221569
chicken anti-GFP (1/500)	Abcam	Cat# ab13970; RRID: AB_300798
mouse anti-Ppy (clone 23-2D3)	IBL	Cat# 10501
mouse anti-Ppy (1/1000)	R&D Biosystems	Cat# MAB62971; RRID: AB_11127208
Alexa 568, 488, 647 and 405 Secondary Ab	Molecular Probes	N/A
Cy3, Cy5, FITC and TRITC Secondary Ab	Southern Biotech	N/A
Critical commercial assays		
Qiagen RNeasy Micro Kit	Qiagen	Catalog # 74004
Qiagen QuantiTect Reverse Transcription Kit	Qiagen	Catalog # 205311
Experimental models: Organisms/strains		
Mouse: Glucagon Promoter-rtTA;TetO-Cre;R26-YFP	Thorel et al., 2010	https://doi.org/10.1038/nature08894
Mouse: Somatostatin Promoter-rtTA;TetO-Cre;R26-YFP	Cigliola et al., 2018	https://doi.org/10.1038/s41556-018-0216-y
Mouse: Mouse Insulin promoter-rtTA;TetO-Cre;R26-YFP	Kusminski et al., 2016	https://doi.org/10.2337/db15-1323
Mouse: Pancreatic Polypeptide promoter-rtTA;TetO-Cre;R26-YFP	Perez-Frances et al., 2021	https://doi.org/10.1038/s41467-021-24788-0
Oligonucleotides		
qPCR primers for hormones and Cre recombinase, See Table S2	This paper	N/A
Software and algorithms		
Prism v8.0.1 software	N/A	https://www.graphpad.com/scientific-software/prism/
Leica Application Suite X 3.0.2.16120	Leica Microsystems	https://www.leica-microsystems.com/products/microscope-software/p/leica-las-x-ls/

RESOURCE AVAILABILITY

Lead contact

Further information and requests for resources and reagents should be directed to and will be fulfilled by the lead contact, Dr. Pedro Luis Herrera (pedro.herrera@unige.ch).

Material availability

This study did not generate new unique reagents.

Data and code availability

- All data reported in this paper will be shared by the lead contact upon request. Microscopy data reported in this paper will be shared by the lead contact upon request.
- This paper does not report original code.
- Any additional information required to reanalyze the data reported in this paper is available from the lead contact upon request.

EXPERIMENTAL MODEL AND SUBJECT DETAILS

Animal models

Transgenic mice were described in earlier studies (Sst-YFPi (Cigliola et al., 2018); Gcg-YFPi (Thorel et al., 2010); Ppy-YFPi (Perez-Frances et al., 2021); Mip-YFPi (Kusminski et al., 2016)). In brief, the reverse tetracycline transactivator sequence (rtTA) was inserted downstream of the endogenous *Sst* and *Ppy* promoters in SST-rtTA and PPY-rtTA knock in lines, respectively. For MIP-rtTA and GLU-rtTA transgenic mice, insulin and glucagon promoter fragments were respectively used to drive the expression of rtTA. Each rtTA line was then bred with TetO-Cre and Rosa26-STOP-YFP transgenic animals to generate experimental mice allowing inducible lineage tracing of the different hormone-expressing islet cell types. Mice were housed in open cages with density varying depending on the size of the cage, in accordance with the Swiss regulation (Cage type S to L, Charles River). Cages were enriched with bedding, nestlet and a mouse house. Temperature and humidity in the housing room was maintained between 20°C to 24°C and 30% to 70%, respectively. The day-night cycles were programmed by alternating 12 h day - 12 h night. Animals received food and tap water ad libitum.

Male and female mice of multiple developmental ages were used in all experiments, as indicated in the results section and figure legends. Animals were randomly allocated to control or treatment groups. Only the mice with the appropriate experimental genotype were used. This study is compliant with ethical regulations regarding animal research, all experiments have been approved and performed according to the guidelines of the Direction générale de la santé du Canton de Genève (license numbers: GE/111/17, GE/121/17, GE/104/20 and GE15820). The mice were randomly selected for treatment and control. Multiple litters were used per experiment and condition.

METHOD DETAILS

Doxycycline

Doxycycline (1 mg/ml; Sigma) was administered in drinking water. The doxycycline solution was changed twice per week.

Islet isolation and RNA extraction

Before islet isolation, pancreas tissue was digested using 2mg/ml Collagenase IV (Sigma, #C7657) at 37°C water bath for 11–12 min. Islet isolation was performed using Histopaque-1119 (Sigma, # 11,191) gradient protocol. Isolated islets were frozen in RLT buffer (Qiagen) with β-mercaptoethanol and stored at −80°C before being processed for RNA extraction. RNA extraction from islets was prepared using the Qiagen RNeasy Micro Kit.

RT-qPCR

cDNA was generated using the Qiagen QuantiTect Reverse Transcription Kit. The resulting cDNA was submitted to q-PCR reaction using the appropriate primer mixes for each gene as well as the Universal qPCR SuperMix component provided in the PowerUp™ SYBR™ Green Master Mix (ThermoFisher # A25742). We used the CorbettRobotics4 robot and the PCR reaction was completed in the CorbettResearch6000 series cycler using a 40 cycles program. Normalization and analysis of data were done with the RT-PCR analysis macro v1.1 (courtesy of the NCCR Genomic Platform, University of Geneva) using 2 different normalization genes (β-*actin* and *Gapdh*) (Cigliola et al., 2018; Chera et al., 2014; Thorel et al., 2010). Samples were run in triplicate. Primers sequences are shown in Table S2.

Immunofluorescence

Cryostat section were 10μm thick. The primary antibodies used were: guinea pig anti-porcine insulin (1/400; DAKO), rabbit anti-insulin (1/3000; Molecular Probes), mouse anti-glucagon (1/1000; Sigma), rabbit anti-glucagon (1/200; DAKO), mouse anti-somatostatin (1/200; BCBC Ab1985), rabbit anti-somatostatin (1/200; DAKO), goat anti-somatostatin (1/200; Santa Cruz Biotechnology), rabbit anti-GFP (1/400; Molecular Probes), chicken anti-GFP (1/500; Abcam), mouse anti-Ppy (1/200; IBL, 23-2D3) and mouse anti-Ppy (1/1000; R&D Biosystems and Abcam). Secondary antibodies were coupled to Alexa 488, 405, 568, 647 (1/500; Molecular

Probes) or TRITC, FITC, Cy3 and Cy5 (1/500; Southern Biotech). All antibodies are listed in Table S1. Sections were also stained with DAPI. All sections were examined with a confocal microscope (Leica TCS SPE).

Ventral or dorsal regions of the pancreas were analyzed based on cell abundance.

QUANTIFICATION AND STATISTICAL ANALYSIS

Error bars represent s. e.m., as indicated in the figure legends. Statistical analyses were performed using Prism v8.0.1 software applying Mann-Whitney tests for comparison. p values are described in Figure Legends. More than three mice per condition and experiment were analyzed as indicated in the Figure Legends and Supplementary Tables. Different litters were analyzed in each experiment. Immunofluorescence was performed more than once for each mouse with >4 cryo-sections/mouse.

Cell Reports, Volume *38*

Supplemental information

Adult pancreatic islet endocrine cells emerge as fetal hormone-expressing cells

Marta Perez-Frances, Maria Valentina Abate, Delphine Baronnier, Philipp E. Scherer, Yoshio Fujitani, Fabrizio Thorel, and Pedro L. Herrera

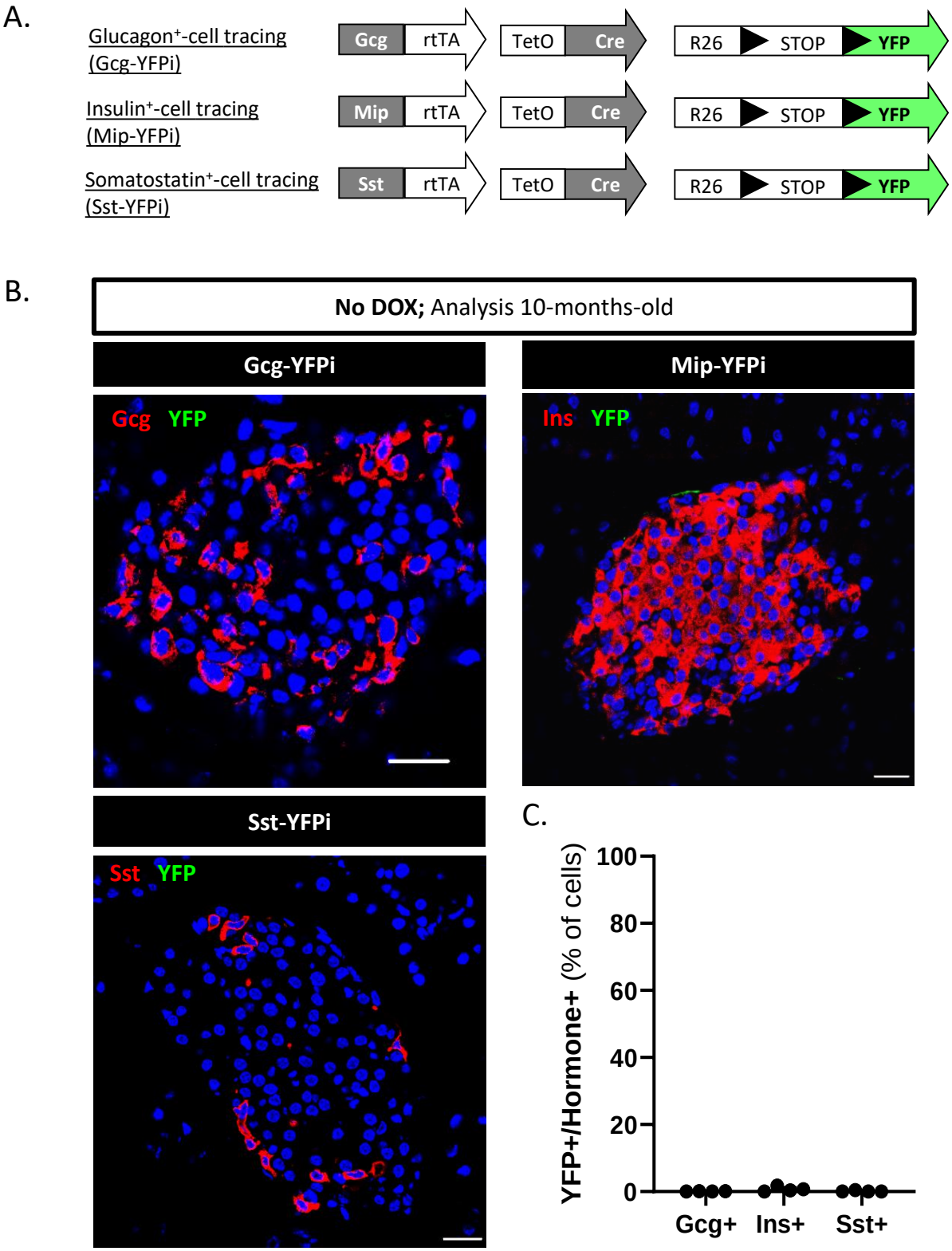

Supplementary Figure 1. Long-term inducible islet cell lineage-tracing systems, related to Figure 1. a, Transgenes required for tracing the lineages of Gcg-expressing α-cells, Ins-expressing β-cells and Sst-expressing δ-cells. **b,** No YFP labelling is observed in untreated ten-month-old mice. Immunofluorescence: Gcg-YFPi (Gcg, red; YFP, green), Mip-YFPi (Ins, red; YFP, green) and Sst-YFPi (Sst, red; YFP, green). Scale bars: 20μm. **c,** Percentage of Gcg-, Ins- and Sst-expressing cells labelled with YFP without DOX treatment (Gcg-YFPi, n=4; Mip-YFPi n=4; Sst-YFPi, n=4). One representative biological replicate of an experiment is presented in the micrographs. Experiments were performed two or more times independently under identical or similar conditions.Quantification details are provided as Source Data file (table b).

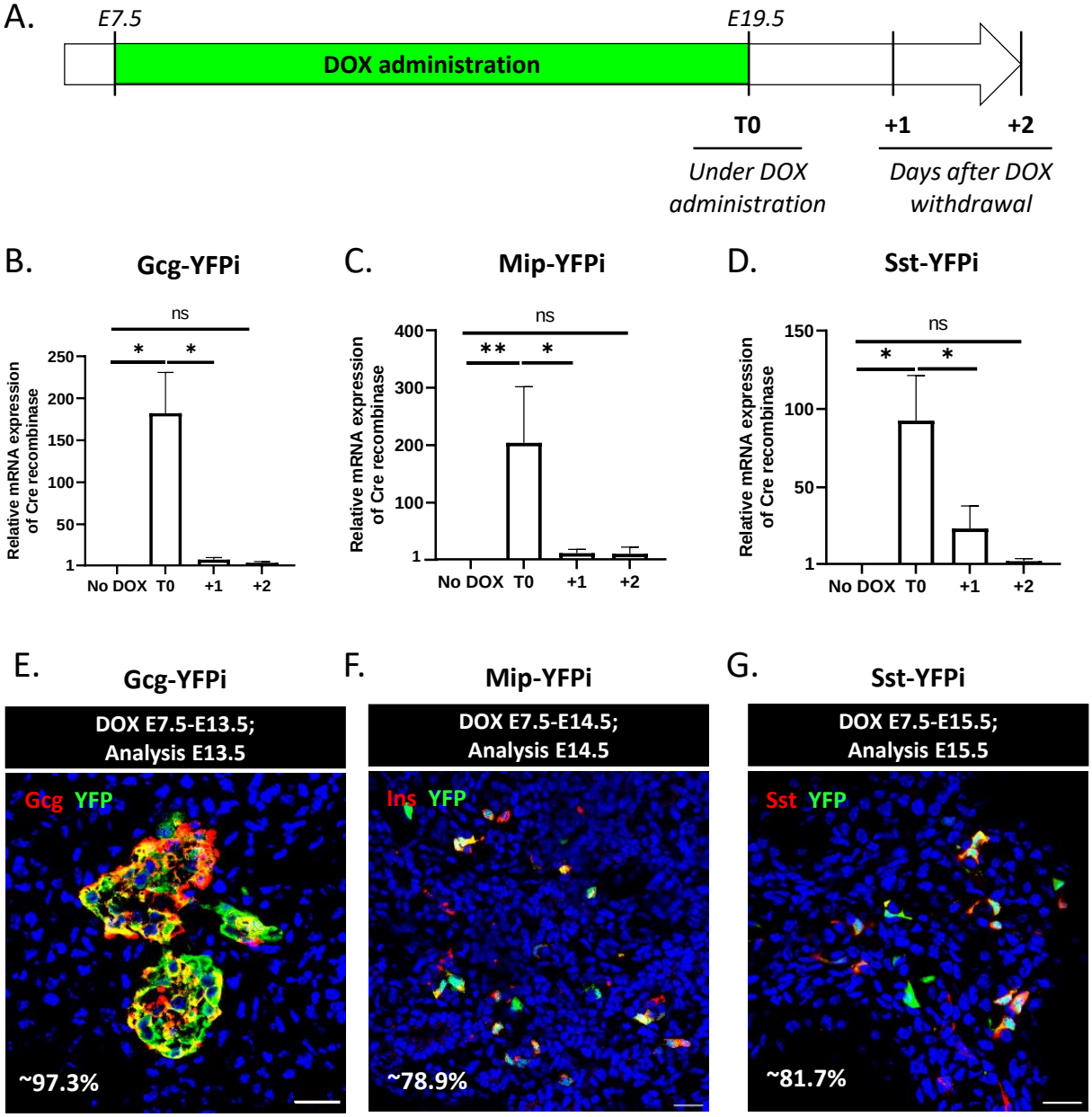

Supplementary Figure 2. A short DOX pulse during pancreas development efficiently labels differentiating hormone+ cells, related to Figure 2. a, Experimental design. DOX administration from E7.5 to E19.5 to pregnant females (T0: under DOX exposure, +1: one day after DOX removal, +2: 2 days after DOX removal). **b-d,** Relative mRNA expression of *Cre* recombinase normalized on hormone expression at different DOX administration timings. Gcg-YFPi: No DOX, n=4; T0, n=4; +1, n=4; +2, n=4 (**b**). Mip-YFPi: No DOX, n=5; T0, n=4; +1, n=4; +2, n=4 (**c**). Sst-YFPi: No DOX, n=4; T0, n=5; +1, n=5; +2, n=6 (**d**). Data are shown as fold change of normalized ct values relative to No DOX (No DOX = 1). Data are presented as mean values ± s.e.m. Two-tailed Mann-Whitney test, P values for Gcg-YFPi: No DOX versus T0: *P* value = 0.0286, T0 versus +1: *P* value = 0.0286, No DOX versus +2: *P value* = 0.20; P values for Mip-YFPi: No DOX versus T0: *P* value = 0.0048, T0 versus +1: *P* value = 0.0286, No DOX versus +2: *P value* = 0.20; P values for Sst-YFPi: No DOX versus T0: *P* value = 0.0357, T0 versus +1: *P* value = 0.0317, No DOX versus +2: *P value* = 0.5357. **e-g.** Labelling efficiency in embryos at E13.5, E14.5 or E15.5 for the Gcg-YFPi (**e;** red, Gcg; green, YFP), Mip-YFPi (**f;** red, Ins; green, YFP) and Sst-YFPi (**g;** red, Sst; green, YFP), respectively. Scale bars: 20μm. Region of the pancreas: whole pancreas. One representative biological replicate of an experiment is presented in the micrographs. Experiments were performed two or more times independently under identical or similar conditions. Quantification details are provided as Source Data file (tables d, e).

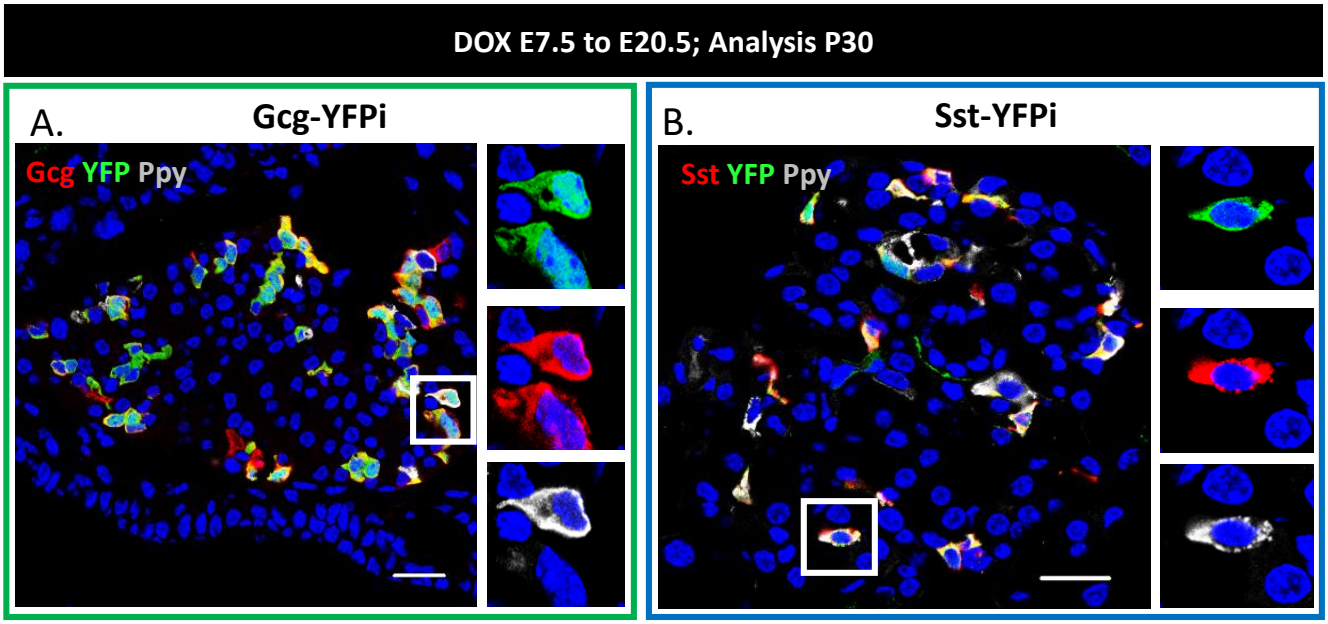

C.

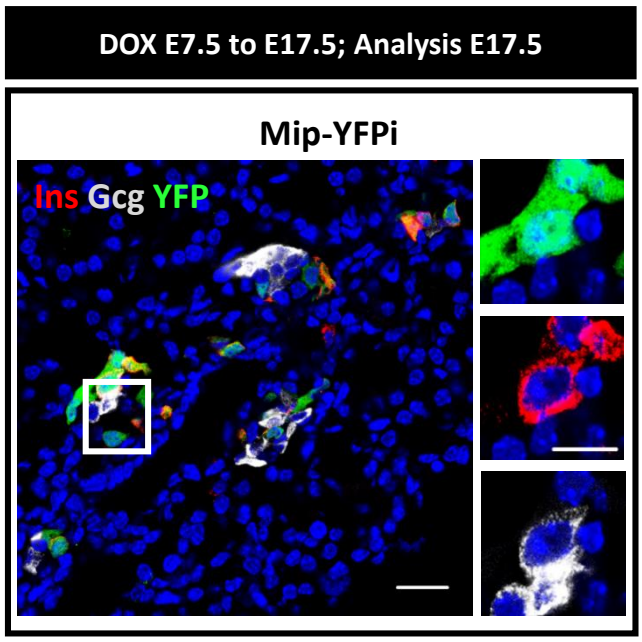

D.

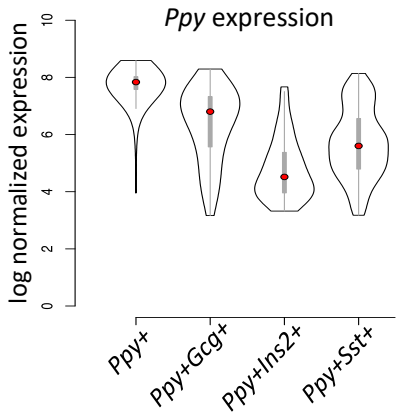

Cell Type	Mean *Ppy* expr	P-adj
Ppy+	7,74	-
Ppy+Gcg+	6,35*	2,30E-126
Ppy+Ins2+	4,81*	2,24E-37
Ppy+Sst+	5,68*	2,14E-114

* Significantly lower as compared to monohormonal *Ppy*+ cells

Supplementary Figure 3. YFP-traced bihormonal cells in embryonic and adult pancreatic islets, related to Figure 4. a-b, Immunofluorescence on pancreatic sections from one-month-old Gcg-YFPi (**a**) and Sst-YFPi (**b**) mice. Bihormonal Ppy-Gcg (**a;** Gcg, Red; YFP, green; Ppy, grey) and Ppy-Sst (**b;** Sst, Red; YFP, green; Ppy, grey) cells are detected. Scale bars: 20µm or 10µm (insets 1, 2, 3). Region of the pancreas: Ventral. **c,** Immunofluorescence on E17.5 pancreatic sections from Mip-YFPi mice. One bihormonal Gcg-Ins cell is shown (inset). Ins, Red; YFP, green; Gcg, grey. Scale bars: 20µm or 10µm (insets). One representative biological replicate of an experiment is presented in the micrographs. **d,** Adult bihormonal PPY+ cells display lower *Ppy* mRNA levels than monohormonal PPY+ cells. Log normalized expression of *Ppy* gene in monohormonal PPY+ cells versus bihormonal Ppy+Gcg+, Ppy+Ins2+ and Ppy+Sst+ cells. Experiments were performed two or more times independently under identical or similar conditions.